Physica B 404 (2009) 1045–1052

Contents lists available at ScienceDirect

Physica B

journal homepage: www.elsevier.com/locate/physb

The bianisotropic medium model for left-handed metamaterials and numerical calculation of negative electromagnetic parameters

Quanhong Fu, Xiaopeng Zhao *

Department of Applied Physics, Northwestern Polytechnical University, Xi'an 710072, PR China

ARTICLE INFO

Article history:
Received 13 April 2008
Received in revised form
2 November 2008
Accepted 4 November 2008

PACS:
41.20.Jb
42.25.Bs
78.20.Ci

Keywords:
LHMs
Bianisotropic medium model
Numerical calculation
Electromagnetic parameters

ABSTRACT

We introduce the bianisotropic medium model into left-handed metamaterials (LHMs). Based on the model, we propose a novel method, which differs from *S*-parameter retrieval method, to calculate the constitutive parameters of LHMs. Via the numerical calculation of permeability μ and permittivity ε, the relation between resonance intensity and geometric parameters for arrays of hexagonal split-ring resonators (SRRs) is acquired. The dendritic structure allows for negative permeability μ in the frequency range of 7.6–9.4 GHz, which is in good agreement with experimental results. The permittivity spectra of arrays of continuous and cut wires reveal the plasmonic and ideal resonant responses, respectively. Moreover, the recovered permittivity ε is free from antiresonance, which is consistent with physical laws.

1. Introduction

Electric permittivity ε and magnetic permeability μ are two fundamental electromagnetic parameters describing the electromagnetic responses of continuous medium. In 1968, substances with simultaneously negative values of ε and μ were studied theoretically by Veselago and referred to as LHMs (left-handed metamaterials) [1]. In 1996, Pendry et al. demonstrated theoretically that the array of metallic wires had negative ε as the frequency of electromagnetic wave is below the plasmonic frequency [2]. The interest in Veselago's work was renewed since Pendry et al. proved theoretically in 1999 that the array of SRRs (split-ring resonators) possessed negative μ in a narrow frequency region [3]. Based on Pendry's suggestion and targeting the original idea of Veselago, Shelby et al. realized LHMs and demonstrated negative refraction in microwave band in 2001 [4], greatly promoting researches on LHMs. Negative permeability metamaterials at THz, 100 THz, and optical frequency were prepared [5–7], highly boosting the magnetic response frequency. The effect of magnetoelectric coupling was studied for explaining the peculiar propagation of electromagnetic wave through negative permeability and LHMs [8,9]. Zhao et al. examined the defect effects in negative permeability and LHMs [10–14] and the magnetic response of dendritic structures at infrared frequencies [15].

Generally, the characteristic transmission spectrum with a pass band in the stop band is thought to be a sign of LHMs [16]. However, the transmission behavior of LHMs is merely the exterior property as several materials have transmission spectrum analogous to that of LHMs but are not left-handed [17]. Therefore, if the left-handed characteristics of a material need to be exactly validated, it is necessary to obtain the negative permittivity ε and permeability μ. For the direct characterization of metamaterials, Smith et al. presented a convenient method, i.e. *S*-parameter retrieval method, to determine ε and μ [18]. *S*-parameter retrieval method is widely used at present, but there exist some shortcomings, e.g. the difficulty in selecting the correct branch of arccosine function and the antiresonance in the recovered electromagnetic parameters. Chen et al. improved the standard retrieval method, but the shortcomings are not thoroughly eliminated [19]. In this work, we introduce bianisotropic medium model into LHMs. Based on the model, another retrieval method, which differs from *S*-parameter retrieval method, is proposed to calculate the constitutive parameters of LHMs. By numerical calculation of ε and μ, we study the electromagnetic responses of metamaterials. The retrieval method proposed in this paper is free from the shortcomings of *S*-parameter retrieval method and has low error sensitivity.

* Corresponding author.
E-mail address: xpzhao@nwpu.edu.cn (X. Zhao).

0921-4526/$ - see front matter © 2008 Elsevier B.V. All rights reserved.
doi:10.1016/j.physb.2008.11.030

2. The bianisotropic medium model for LHMs and calculation method for constitutive parameters

Any artificial structured metamaterial can be considered as bianisotropic medium when the wave length in the metamaterial is much larger than the dimensions and spacing of the constituent scattering inclusions that compose the medium, and the electromagnetic responses are completely described by the constitutive parameters. LHMs as well as negative permeability or permittivity metamaterials usually satisfy the wave length limitation, and can be described in terms of the bianisotropic constitutive relations [20]

$$\begin{cases} \boldsymbol{D} = \bar{\bar{\varepsilon}}\varepsilon_0\boldsymbol{E} + j\sqrt{\varepsilon_0\mu_0}\,\bar{\bar{\chi}}^{\mathrm{T}}\boldsymbol{H} \\ \boldsymbol{B} = \bar{\bar{\mu}}\mu_0\boldsymbol{H} - j\sqrt{\varepsilon_0\mu_0}\,\bar{\bar{\chi}}\boldsymbol{E} \end{cases} \tag{1}$$

where $\bar{\bar{\varepsilon}}$, $\bar{\bar{\mu}}$ and $\bar{\bar{\chi}}$ are effective dielectric permittivity, magnetic permeability and magnetoelectric coupling coefficient, respectively. Note that the $\bar{\bar{\chi}}$ describes the contribution of electric and magnetic field to magnetization and polarization, respectively, and is related with the property of chirality. $\bar{\bar{\varepsilon}}$, $\bar{\bar{\mu}}$ and $\bar{\bar{\chi}}$ can be easily expressed in terms of the polarizabilities $\overline{\overline{a_{ee}}}$, $\overline{\overline{a_{mm}}}$,$\overline{\overline{a_{em}}}$ and $\overline{\overline{a_{me}}}$ of inclusion. The detailed derivation is as follows:

The macroscopic properties of a medium are described by its polarization $\boldsymbol{P}$ and magnetization $\boldsymbol{M}$ vectors

$$\begin{cases} \boldsymbol{D} = \varepsilon_0\boldsymbol{E} + \boldsymbol{P} = \varepsilon_0\boldsymbol{E} + N\boldsymbol{p} \\ \boldsymbol{B} = \mu_0(\boldsymbol{H} + \boldsymbol{M}) = \mu_0(\boldsymbol{H} + N\boldsymbol{m}) \end{cases} \tag{2}$$

where $\boldsymbol{p}$ and $\boldsymbol{m}$ represent induced electric and magnetic dipole moments of inclusion, i.e.

$$\begin{cases} \boldsymbol{p} = \dfrac{1}{-j\omega}\oiint \boldsymbol{J}_S\,\mathrm{d}S \\ \boldsymbol{m} = \dfrac{1}{2}\oiint \boldsymbol{r}\times\boldsymbol{J}_S\,\mathrm{d}S \end{cases} \tag{3}$$

(the time convention $e^{-j\omega t}$ is assumed) and N is the inclusion number per unit volume.

For a linear medium, $\boldsymbol{p}$ and $\boldsymbol{m}$ can be related with local field $\boldsymbol{E}_{loc}$ and $\boldsymbol{H}_{loc}$ by the following linear relations:

$$\begin{cases} \boldsymbol{p} = \varepsilon_0(\overline{\overline{a_{ee}}}\boldsymbol{E}_{loc} + \overline{\overline{a_{em}}}\eta\boldsymbol{H}_{loc}) \\ \boldsymbol{m} = \overline{\overline{a_{mm}}}\boldsymbol{H}_{loc} + \overline{\overline{a_{me}}}\boldsymbol{E}_{loc}/\eta \end{cases} \tag{4}$$

where $\overline{\overline{a_{ee}}}$, $\overline{\overline{a_{mm}}}$, $\overline{\overline{a_{em}}}$ and $\overline{\overline{a_{me}}}$ are the polarizability dyadics of inclusion and $\eta = (\mu_0/\varepsilon_0)^{1/2}$ is the wave impedance of free space.

Considering the Lorentzian field, we can write

$$\begin{cases} \boldsymbol{E}_{loc} = \boldsymbol{E} + \boldsymbol{P}/(3\varepsilon_0) \\ \boldsymbol{H}_{loc} = \boldsymbol{H} + \boldsymbol{M}/3 \end{cases} \tag{5}$$

The relation above is true for cubic lattice; for other highly symmetric lattices, it is still approximately applicable because the electromagnetic interactions between adjoining scattering elements cancel each other.

Combining expressions (4) and (5), $\boldsymbol{P}$ and $\boldsymbol{M}$ are expressed as functions of $\boldsymbol{E}$ and $\boldsymbol{H}$. Results are put in expression (2), and the obtained formulas are compared with general constitutive relations (1). Then expressions of $\bar{\bar{\varepsilon}}$, $\bar{\bar{\mu}}$ and $\bar{\bar{\chi}}$ can be derived:

$$\begin{cases} \bar{\bar{\varepsilon}} = \bar{\bar{I}} + \overline{\overline{K_1}}^{-1}\left[N\overline{\overline{a_{ee}}} + \dfrac{N^2}{3}\overline{\overline{a_{em}}}\left(\bar{\bar{I}} - \dfrac{N\overline{\overline{a_{mm}}}}{3}\right)^{-1}\overline{\overline{a_{me}}}\right] \\ \bar{\bar{\mu}} = \bar{\bar{I}} + \overline{\overline{K_2}}^{-1}\left[N\overline{\overline{a_{mm}}} + \dfrac{N^2}{3}\overline{\overline{a_{me}}}\left(\bar{\bar{I}} - \dfrac{N\overline{\overline{a_{ee}}}}{3}\right)^{-1}\overline{\overline{a_{em}}}\right] \\ \bar{\bar{\chi}} = j\overline{\overline{K_2}}^{-1}N\overline{\overline{a_{me}}}\left[\bar{\bar{I}} + \left(\bar{\bar{I}} - \dfrac{N\overline{\overline{a_{ee}}}}{3}\right)^{-1}\dfrac{N\overline{\overline{a_{ee}}}}{3}\right] \end{cases} \tag{6}$$

where $\bar{\bar{I}}$ is unit dyadic, and

$$\begin{cases} \overline{\overline{K_1}} = \bar{\bar{I}} - \dfrac{N\overline{\overline{a_{ee}}}}{3} - \dfrac{N^2}{9}\overline{\overline{a_{em}}}\left(\bar{\bar{I}} - \dfrac{N\overline{\overline{a_{mm}}}}{3}\right)^{-1}\overline{\overline{a_{me}}} \\ \overline{\overline{K_2}} = \bar{\bar{I}} - \dfrac{N\overline{\overline{a_{mm}}}}{3} - \dfrac{N^2}{9}\overline{\overline{a_{me}}}\left(\bar{\bar{I}} - \dfrac{N\overline{\overline{a_{ee}}}}{3}\right)^{-1}\overline{\overline{a_{em}}} \end{cases} \tag{7}$$

If $\overline{\overline{a_{ee}}}$, $\overline{\overline{a_{mm}}}$, $\overline{\overline{a_{em}}}$, $\overline{\overline{a_{me}}}$ and N are obtained, $\bar{\bar{\varepsilon}}$, $\bar{\bar{\mu}}$ and $\bar{\bar{\chi}}$ can be computed. Usually, N is known, but $\overline{\overline{a_{ee}}}$, $\overline{\overline{a_{mm}}}$, $\overline{\overline{a_{em}}}$and $\overline{\overline{a_{me}}}$ must be extracted from expressions (3) and (4) by numerical method. The study under six different incidences is needed to obtain all the components of the four polarizability tensors. For each configuration, current distribution is solved by using Computer Simulation Technology Microwave Studio (CST MWS, an electromagnetic field simulation software based on finite integration technology for electromagnetic analysis and design in the high frequency range), and then $\boldsymbol{p}$ and $\boldsymbol{m}$ vectors are evaluated using integrals in expression (3). Considering all the equations for all the components of dipole moments, we get 36 scalar equations and need to determine the 36 terms of polarizability dyadics. The particular choice of the six incidences ($\boldsymbol{k}\|\pm x$, $\boldsymbol{E}\|y$, $\boldsymbol{H}\|z$; $\boldsymbol{k}\|\pm y$, $\boldsymbol{E}\|z$, $\boldsymbol{H}\|x$; $\boldsymbol{k}\|\pm z$, $\boldsymbol{E}\|x$, $\boldsymbol{H}\|y$. The coordinate system is indicated in Fig. 1) gives a very easy way to solve the system of equations. The physical requirements, especially reciprocal properties, imposed on the components of the dyadics give $\overline{\overline{a_{ee}}} = \overline{\overline{a_{ee}}}^{\mathrm{T}}$, $\overline{\overline{a_{mm}}} = \overline{\overline{a_{mm}}}^{\mathrm{T}}$ and $\overline{\overline{a_{em}}} = -\overline{\overline{a_{me}}}^{\mathrm{T}}$.

In view of the symmetry of elements (see Fig. 1), we can neglect the magnetoelectric coupling, i.e. $\overline{\overline{a_{em}}} = \overline{\overline{a_{me}}} = 0$, and therefore $\bar{\bar{\chi}} = 0$. As a matter of convenience, the coordinate axes are selected along three special orthogonal directions (usually the symmetry axes of inclusions, see Fig. 1) to assure that $\overline{\overline{a_{ee}}}$ and $\overline{\overline{a_{mm}}}$ are diagonal, and accordingly $\bar{\bar{\varepsilon}}$ and $\bar{\bar{\mu}}$ are also diagonal. The microwave propagates in the direction of x axis with the electric

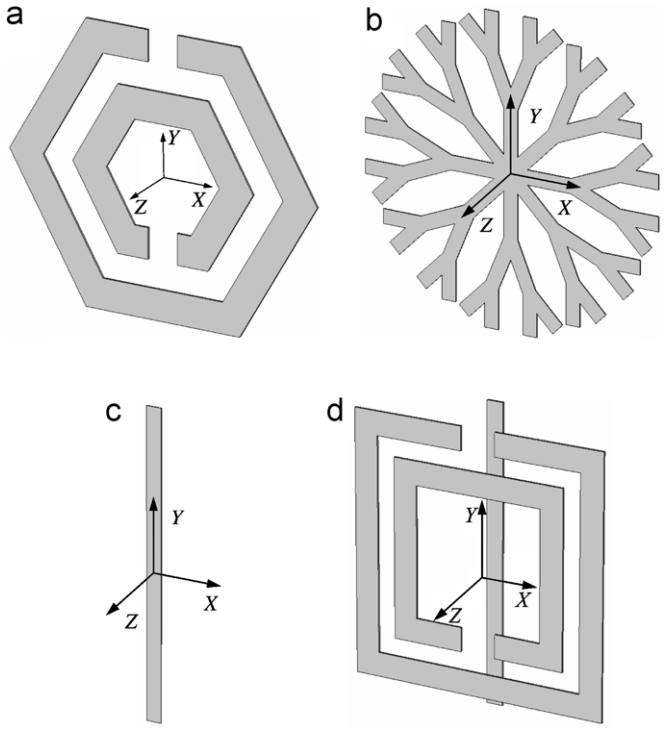

Fig. 1. Orientations of inclusions in space: (a) hexagonal SRR; (b) dendritic structure; (c) wire; and (d) element of LHMs. The incident wave propagates along the x axis with the electric and magnetic field polarized along the y and z axes, respectively.

and magnetic field polarized along the y and z directions, respectively. For the specific orientation of incident wave with respect to rings and wires in this paper, all the components of $\overline{\overline{\varepsilon}}$ and $\overline{\overline{\mu}}$ are not needed to understand the polarization and magnetization properties of metamaterials. On the contrary, only two components are needed. Because the electric field $\boldsymbol{E}$ and magnetic field $\boldsymbol{H}$ have only y and z components, and yield polarization and magnetization along y and z axes, respectively, which can be fully described by the components ε_{yy} and μ_{zz}, the propagation properties of electromagnetic wave in metamaterials can be determined by the following components:

$$\begin{cases} \varepsilon_{yy} = 1 + Na_{eeyy}/(1 - Na_{eeyy}/3) \\ \mu_{zz} = 1 + Na_{mmzz}/(1 - Na_{mmzz}/3) \end{cases} \quad (8)$$

and have nothing to do with the other components of $\overline{\overline{\varepsilon}}$ and $\overline{\overline{\mu}}$. For simplicity, we use ε and μ to denote the components ε_{yy} and μ_{zz} of $\overline{\overline{\varepsilon}}$ and $\overline{\overline{\mu}}$, respectively, in what follows. Therefore, once a_{eeyy} and a_{mmzz} of element are obtained, the electromagnetic responses of metamaterials can be understood completely.

In the afore mentioned calculation procedure of electromagnetic parameters, there is no arccosine operation and extraction of square root as in S-parameter retrieval method [18], so there does not exist the problem of the branch selection of arccosine function and the unreasonable discontinuities in the retrieved parameters.

In S-parameter retrieval method, the position of effective boundaries of slab affects the phase of transmitted and reflected wave, and consequently influences the value of ε and μ. Therefore, the position of effective boundaries has to be accurately

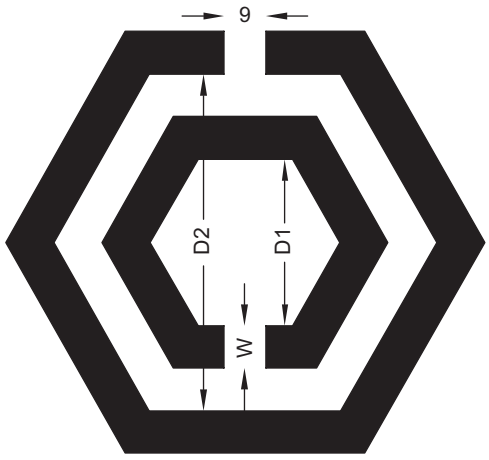

Fig. 2. Geometric parameters of hexagonal copper SRRs. The metal depth of hexagonal SRRs is $d = 0.02$ mm. The lattice constants of array of hexagonal SRRs along x, y and z directions are a, b, and c, respectively.

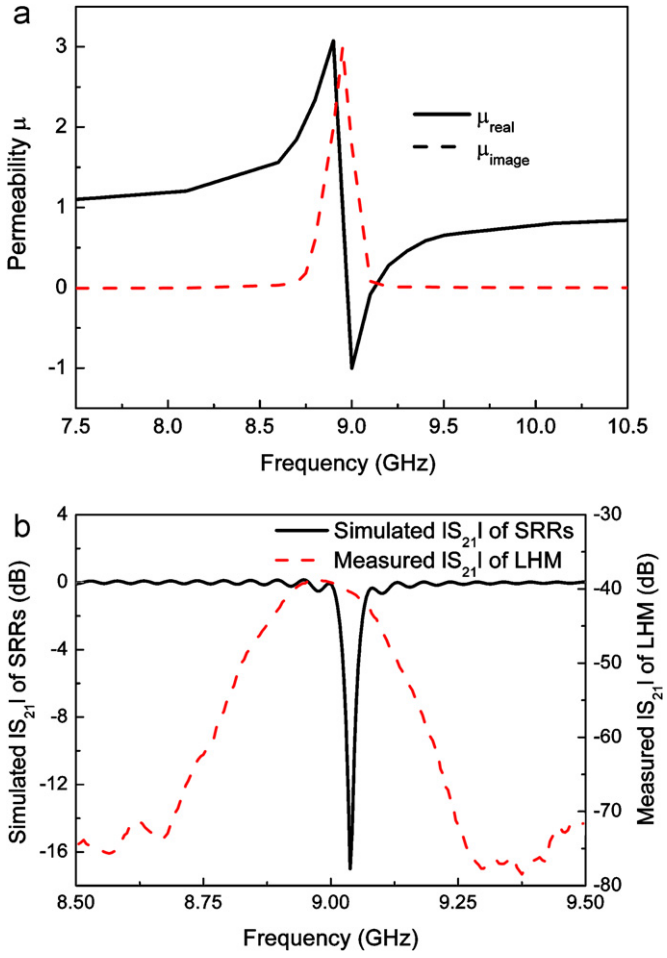

Fig. 3. (a) Calculated frequency dependence of permeability of standard array of hexagonal SRRs and (b) simulated transmission of standard array of hexagonal SRRs (solid line) and measured transmission of combined system of hexagonal SRRs and continuous copper wires, i.e. LHM (dash line). The continuous copper wires have a width of 0.5 mm and a metal depth of 0.02 mm.

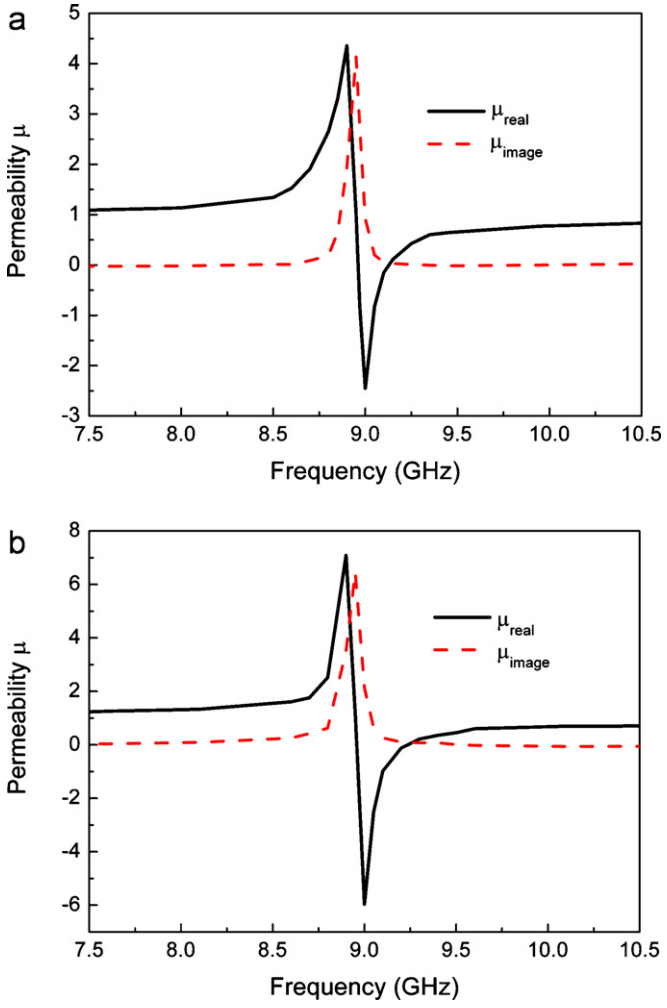

Fig. 4. Permeability as a function of frequency when changing $D1/D2$ and ε_b: (a) $D1/D2 = 1.8/3.4$ mm, $\varepsilon_b = 2.45$ and (b) $D1/D2 = 2.6/4.2$ mm, $\varepsilon_b = 1.25$.

determined to obtain the correct value of ε and μ. In the calculation method presented in this paper, however, the value of ε and μ is mainly dependent on the induced current and the local field, and independent of the position of effective boundaries. As a result, the problem of effective boundaries can be avoided.

In *S*-parameter retrieval method, the intermediate variables n and z, accordingly ε and μ as well, are sensitive to the accuracy of S_{11} and S_{21} within and below the resonance band [19]. In the calculation method presented in this paper, nevertheless, the intermediate variables $\overline{\overline{a_{ee}}}$, $\overline{\overline{a_{mm}}}$, $\overline{\overline{a_{em}}}$ and $\overline{\overline{a_{me}}}$ are not sensitive to the accuracy of induced current [see Eqs. (3) and (4)]. Thus, the permittivity ε and the permeability μ are not sensitive to the accuracy of induced current. It can be concluded that the calculation method presented in this paper has good stability.

3. Numerical results and discussion

3.1. Permeability of arrays of hexagonal SRRs

In this section, we study the influence of geometric parameters of hexagonal copper SRRs on magnetic resonance by numerical calculation of permeability μ. The geometric parameters of hexagonal copper SRRs are indicated in Fig. 2. We utilize the additional degree of freedom in designing metamaterials [21], board dielectric constant ε_b, to keep the resonance frequency constant for it is more significant to tune the electromagnetic responses of metamaterials at fixed operational frequency.

3.1.1. The permeability of standard array of hexagonal SRRs

We take $D1/D2 = 1.0/2.6\,\text{mm}$, $w = 0.3\,\text{mm}$, $g = 0.3\,\text{mm}$, $a \times b \times c = 5 \times 5 \times 5\,\text{mm}^3$, and $\varepsilon_b = 4.65$ as system parameters of the standard array of hexagonal SRRs. The calculated frequency dependence of permeability μ is indicated in Fig. 3(a). To validate the calculated results, we simulate the transmission of standard array of hexagonal SRRs by using CST MWS and measure the transmission of combined system of hexagonal SRRs and continuous copper wires by using AV3618 vector network analyzer in free space. The simulated and measured results are indicated in Fig. 3(b).

Fig. 3(a) shows that the form of calculated permeability of the standard array of hexagonal SRRs is in agreement with the ideal resonant form

$$\mu(\omega) = 1 - \frac{\omega_{mp}^2}{\omega^2 - \omega_0^2 + i\Gamma\omega} \tag{9}$$

where $\omega_0/2\pi = 9.0\,\text{GHz}$, $\omega_{mp}/2\pi = 3.0\,\text{GHz}$, $\Gamma/2\pi = 0.32\,\text{GHz}$ and the standard array of hexagonal SRRs exhibits magnetic resonance around $f = 9.0\,\text{GHz}$, implementing negative permeability, $\mu_{real} = -1.0017$. The solid line in Fig. 3(b) demonstrates

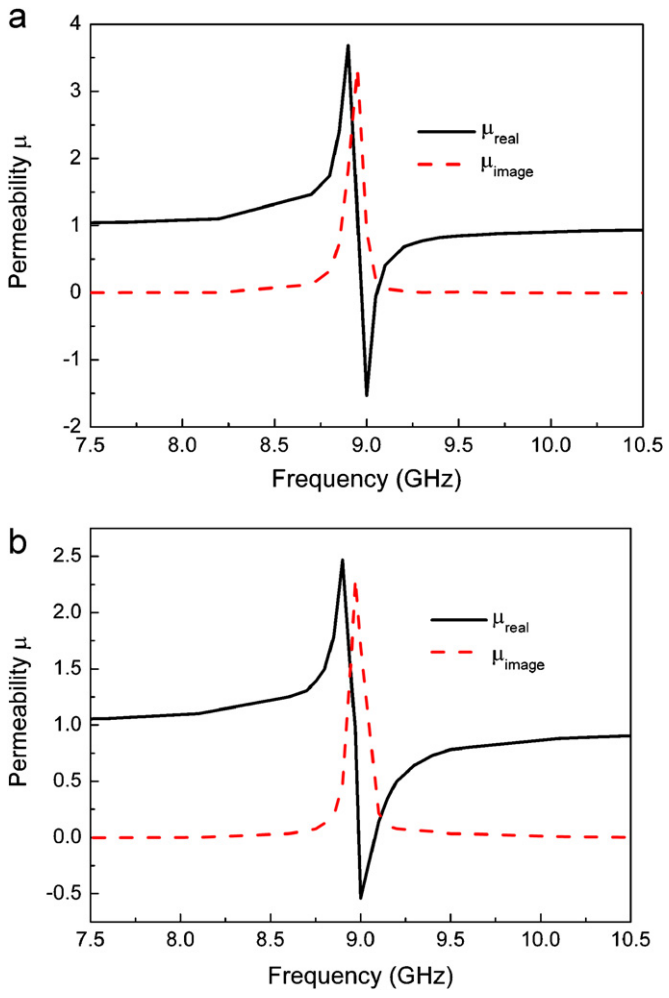

Fig. 5. Permeability versus frequency when altering w and ε_b: (a) $w = 0.2\,\text{mm}$, $\varepsilon_b = 3.65$ and (b) $w = 0.4\,\text{mm}$, $\varepsilon_b = 6.45$.

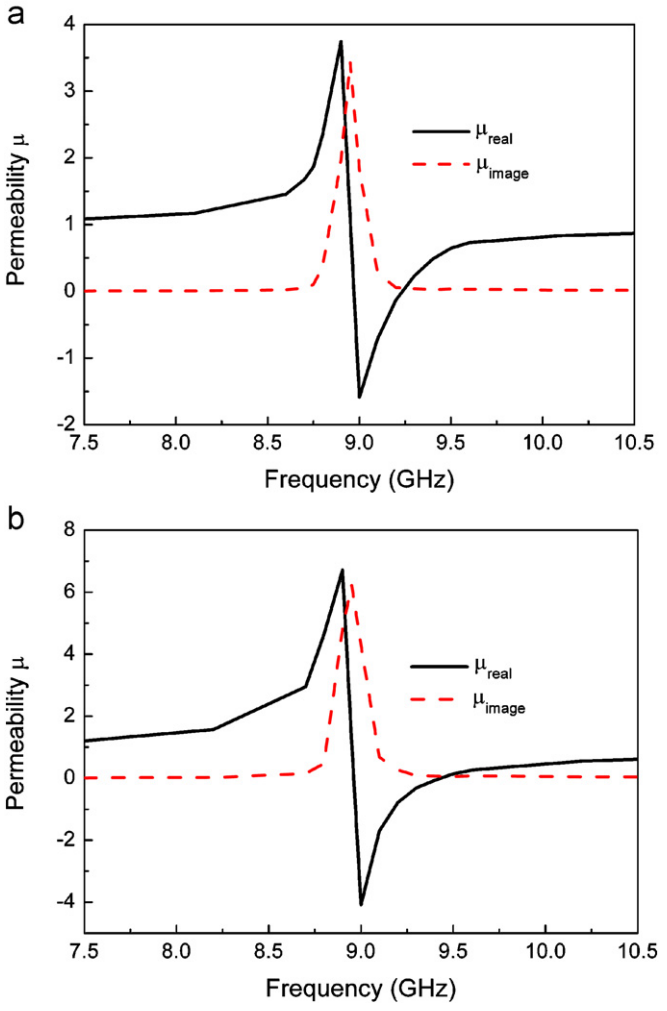

Fig. 6. Frequency dependence of permeability when merely varying the lattice constants: (a) $a \times b \times c = 5 \times 5 \times 3\,\text{mm}^3$ and (b) $a \times b \times c = 5 \times 5 \times 1\,\text{mm}^3$.

that there is a dip around $f = 9.0\,\mathrm{GHz}$ in the transmission spectrum of hexagonal SRRs, implying the existence of magnetic resonance; correspondingly, the dash line exhibits a pass band in the transmission spectrum of combined system of hexagonal SRRs and continuous wires, indicating the left-handed behavior of the combined system, which is consistent with the negative permeability band around $f = 9.0\,\mathrm{GHz}$ in Fig. 3(a).

3.1.2. The influence of $D1/D2$ on resonance intensity

When changing $D1/D2$ of hexagonal SRRs and the board dielectric constant ε_b, the calculated permeability μ as a function of frequency is shown in Fig. 4(a) and (b).

By comparing Fig. 4(a) and (b) with Fig. 3(a), it can be seen that increasing $D1/D2$ of hexagonal SRRs enhances the magnetic resonance and the resonance frequency can stay constant via lowering the board dielectric constant ε_b. This instance can be easily interpreted. When $D1/D2$ increases, the surface area as well as magnetic moment of element increases accordingly, leading to a larger magnetization. Thus, the resonance intensity is enhanced.

3.1.3. The influence of w on resonance intensity

When altering w of hexagonal SRRs and the board dielectric constant ε_b, the calculated permeability μ versus frequency are demonstrated in Fig. 5(a) and (b).

Compared with Fig. 3(a), Fig. 5(a) and (b) shows that reducing w of hexagonal SRRs enhances the magnetic resonance and the resonance frequency can keep constant by lowering the board dielectric constant ε_b. This case can be simply explained. When w reduces, the surface current as well as magnetic moment of element increases correspondingly, resulting in a larger magnetization. Therefore, the resonance intensity is enhanced.

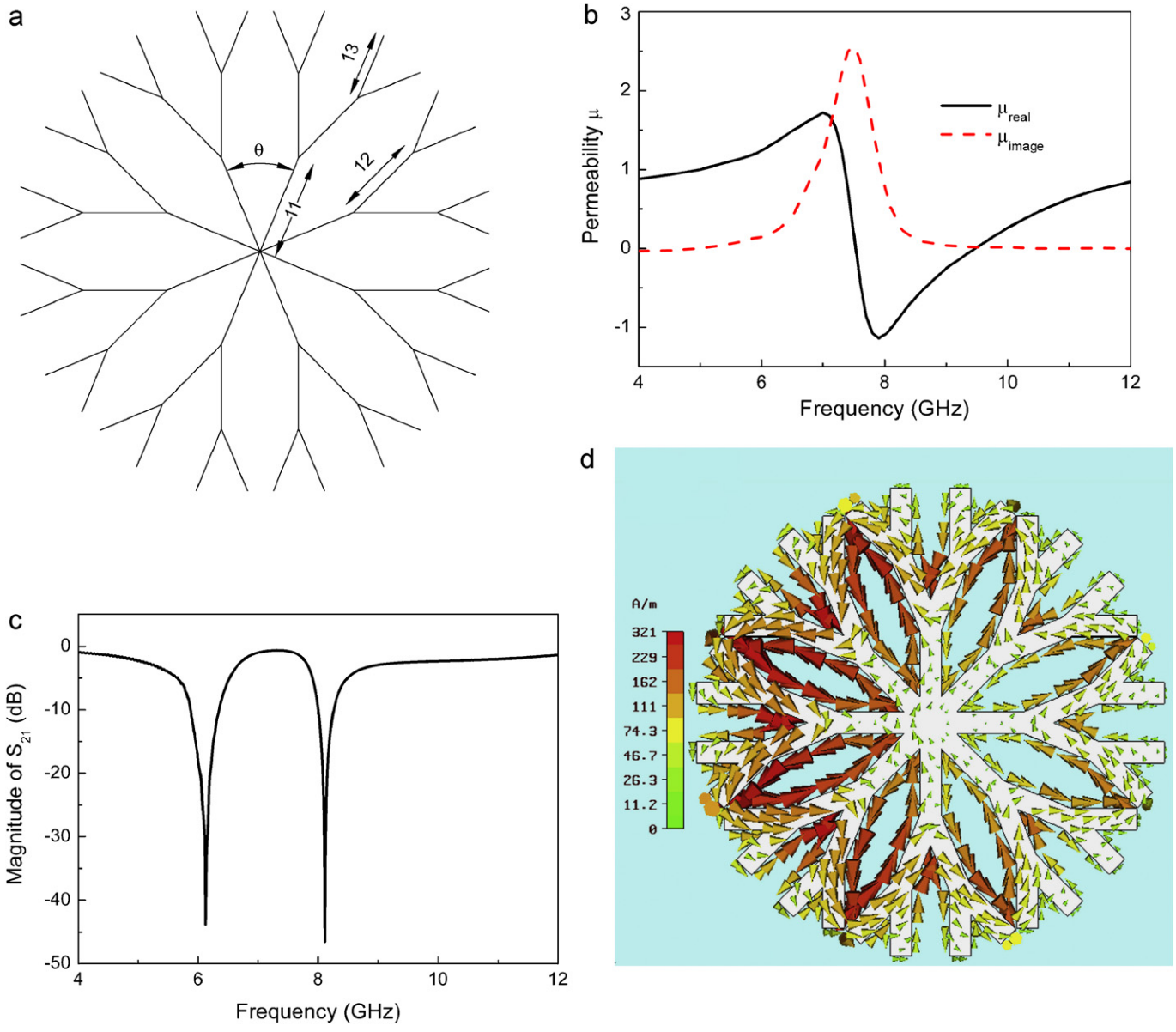

Fig. 7. (a) Geometric parameters of copper dendritic structure. $l1 = 1.32\,\mathrm{mm}$, $l2 = 1.08\,\mathrm{mm}$, $l3 = 0.94\,\mathrm{mm}$, $\theta = 45^\circ$, and $\varepsilon_b = 4.65$. The copper dendritic structures have a linewidth of 0.3 mm and a metal depth of 0.02 mm. The lattice constants along x, y and z directions are $a = 7\,\mathrm{mm}$, $b = 7\,\mathrm{mm}$, and $c = 5\,\mathrm{mm}$, respectively; (b) permeability as a function of frequency of copper dendritic structures; (c) simulated transmission of copper dendritic structures; and (d) (color online) simulated distribution of induced current on the surface of copper dendritic structure at resonance frequency $f = 7.9\,\mathrm{GHz}$.

3.1.4. The influence of lattice constants on resonance intensity

When merely varying the lattice constants of array of hexagonal SRRs, the calculated frequency dependence of permeability μ is indicated in Fig. 6(a) and (b).

By comparing Fig. 6(a) and (b) with Fig. 3(a), it is shown that merely decreasing the lattice constants, i.e. increasing the inclusion number per unit volume N, enhances the magnetic resonance and expands the frequency range where magnetic resonance occurs with resonance frequency maintaining constant. This situation is consistent with electromagnetic theory as well as Pendry's results [3]. According to the magnetization theory of magnetic medium, the increment of N leads to a larger magnetization, and thus the resonance intensity is enhanced; furthermore, Pendry et al. demonstrates that the resonance frequency is independent of N as a result of neglecting the interaction between elements.

3.2. The permeability of array of dendritic structures

The dendritic structure [see Fig. 1(b)] is believed to be a proper model for simplifying the structure of LHMs and increasing the magnetic response frequency. Therefore, we study the magnetic response of copper dendritic structures by calculating the permeability. The geometric parameters of copper dendritic structure are indicated in Fig. 7(a). The calculated permeability μ as a function of frequency is shown in Fig. 7(b). Utilizing CST MWS, we also simulate the transmission behavior of copper dendritic structures and the surface current distribution at resonance frequency. The simulated results are indicated in Fig. 7(c) and (d).

Fig. 7(b) demonstrates that the array of copper dendritic structures exhibits magnetic resonance around $f = 7.9$ GHz, $\mu_{\text{real}} = -1.138$, and the real part of permeability goes negative over the frequency range 7.6–9.4 GHz. Fig. 7(c) shows the transmission spectrum of copper dendritic structures. We can see from Fig. 7(c) that there are two dips in the transmission spectrum, which locate at 6.1 and 8.1 GHz, respectively. Combining the permeability curve in Fig. 7(b) with the transmission spectrum in Fig. 7(c), we conclude that the first dip at 6.1 GHz arises from electric resonance while the second dip at 8.1 GHz owes to magnetic resonance, suggesting the possibility of simultaneously achieving electric and magnetic resonance, i.e. achieving LHMs, by only dendritic structures with appropriate geometric parameters. Fig. 7(d) exhibits the simulated distribution of induced current on the surface of copper dendritic structure at resonance frequency $f = 7.9$ GHz. The intensity of induced current arrives at maximum around resonance frequency. It can be seen from Fig. 7(d) that the induced current is mainly divided into eight ring currents of the same circulating direction which correspond to eight single-ring SRRs. As a result, the eight magnetic moments have the same direction and yield a large net magnetic moment, leading to strong magnetization as well as negative permeability. Virtually, single-ring SRRs also realize negative permeability [22]. Hence, it is in expectation that the combination of single-ring SRRs, i.e. dendritic structures, can realize negative permeability. Moreover, the negative permeability band in Fig. 7(b) is much wider than that of periodic array of constituent single-ring SRRs (the permeability curve of periodic array of constituent single-ring SRRs is analogous to that in Fig. 3(a) and not shown here) because of the various orientations of single-ring SRRs in dendritic structure.

3.3. Permittivity of arrays of copper wires

3.3.1. The permittivity of array of continuous copper wires

As shown in Fig. 1(c), the continuous copper wires have a width of 0.5 mm and a metal depth of 0.02 mm. The lattice constants along x and z directions are $a = 5$ mm and $c = 5$ mm, respectively. In simulation, the ends of continuous copper wires contact the two electric boundaries of unit cell. The calculated permittivity ε versus frequency is indicated in Fig. 8(a).

3.3.2. The permittivity of array of cut copper wires

As shown in Fig. 1(c), the length of cut copper wires is 10 mm. The metal depth and width are the same as those of continuous wires. The lattice constants along x, y and z directions are $a = 5$ mm, $b = 12$ mm, and $c = 5$ mm, respectively. The calculated frequency dependence of permittivity ε is shown in Fig. 8(b).

Fig. 8(a) shows that the electric response of array of continuous wires is similar to that of plasmon with a plasmonic frequency of 14.0 GHz, while Fig. 8(b) demonstrates that the electric resonance response of array of cut wires is analogous to that of ordinary medium caused by bound electrons with a resonance frequency of 12.5 GHz, which is entirely consistent with what were predicted by effective medium theory (see the instances of wire and cut-wire in Fig. 2 of Ref. [17]).

3.4. Permittivity and permeability of LHMs

To compare the method presented in this paper with S-parameter retrieval method, we calculate the permeability μ and permittivity ε of LHMs whose unit cell is indicated in Fig. 2 of

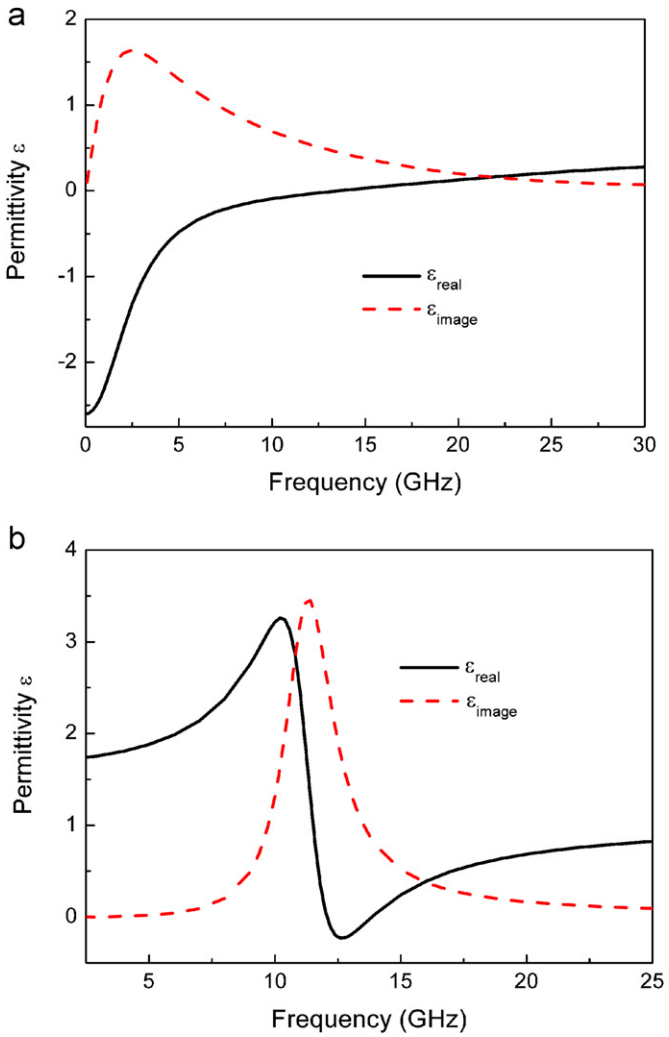

Fig. 8. Frequency dependence of permittivity of arrays of wires: (a) continuous wires and (b) cut wires.

Ref. [23]. The calculated results are demonstrated in Fig. 9(a) and (b). For the convenience of comparison, the retrieved permeability μ and permittivity ε by *S*-parameter retrieval method are shown in Fig. 10(a) and (b).

By comparing Fig. 9 with Fig. 10, it is shown that there is a good match between the two permeability curves [see Figs. 9(a) and 10(a)], but a serious discrepancy between the two permittivity curves [see Figs. 9(b) and 10(b)]. The imaginary part of permittivity in Fig. 10(b) is negative, which is called antiresonance and unphysical. However, the imaginary part of permittivity in Fig. 9(b) is positive, i.e. without antiresonance, which is consistent with physical laws [24]. Therefore, the retrieval method presented in this paper is excellent for determining the electromagnetic parameters of metamaterials, and the artificial structured metamaterials can be well described by the bianisotropic medium model which is based on effective medium theory.

4. Conclusions

The bianisotropic medium model for LHMs has been presented. To study the electromagnetic responses of LHMs, we have proposed a novel method, which differs from *S*-parameter retrieval method, to calculate the effective permeability and permittivity. The main conclusions are as follows:

(1) Increasing the diameters of hexagonal SRRs, reducing the linewidth, and decreasing the lattice constants all enhance the magnetic resonance and the resonance frequency can keep constant by altering the board dielectric constant.
(2) The array of dendritic structures exhibits magnetic resonance around $f = 7.9\,\text{GHz}$, $\mu_{\text{real}} = -1.138$, and the real part of permeability goes negative over the frequency range 7.6–9.4 GHz.
(3) The electric response of array of continuous wires is similar to that of plasmon, while the electric resonance response of array of cut wires is analogous to that of ordinary medium caused by bound electrons.
(4) The calculated permittivity based on bianisotropic medium model is free from antiresonance, which is consistent with physical laws.
(5) The calculation method presented in this paper is free from the problems of the sign selection of square root, the branch choice of multiform function, and the determination of effective boundaries, and has good stability.

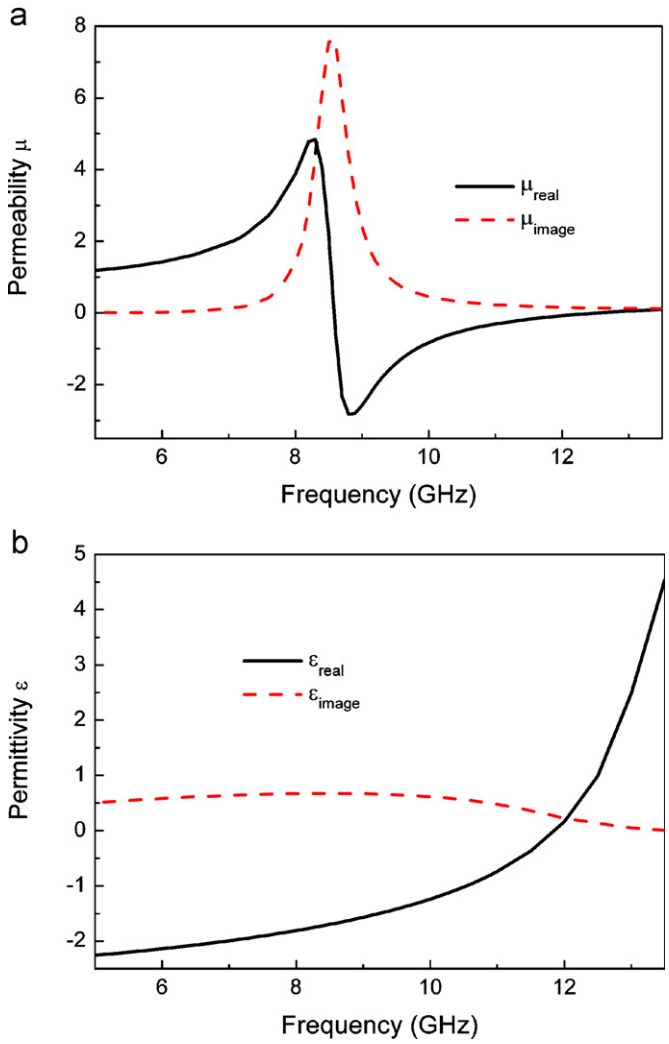

Fig. 9. Calculated permeability and permittivity by the method presented in this paper: (a) permeability as a function of frequency and (b) permittivity as a function of frequency.

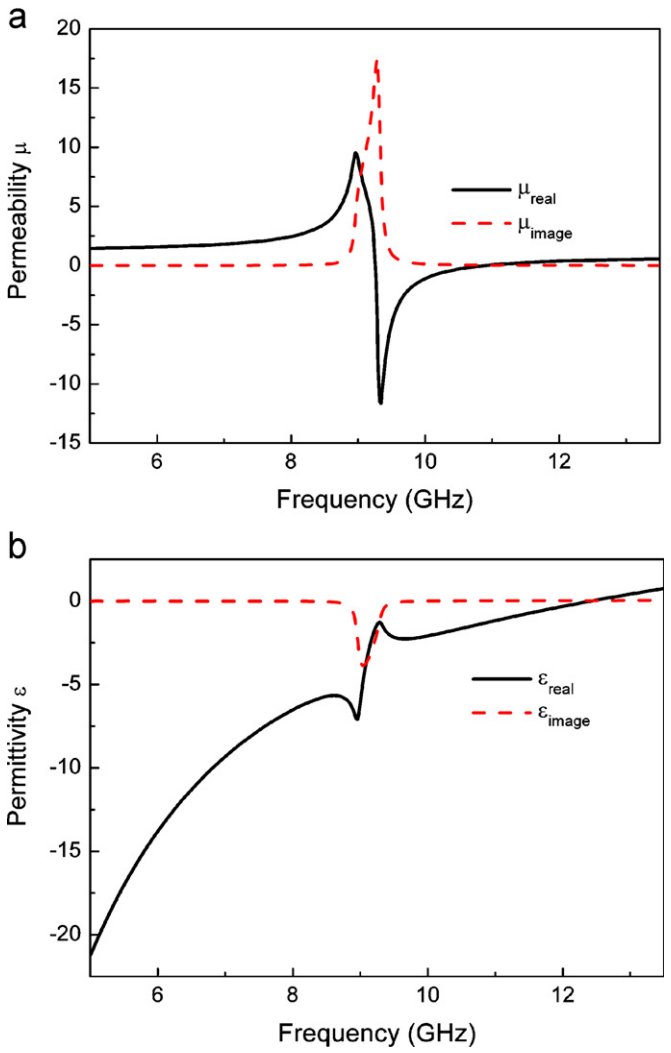

Fig. 10. Retrieved permeability and permittivity by *S*-parameter retrieval method: (a) permeability as a function of frequency and (b) permittivity as a function of frequency.

Acknowledgments

This work was supported by the National Nature Science Foundation of China under Grant nos. 50632030, 50872113 and National Basic Research Program of China under sub-project 2004CB719805.

References

[1] V.G. Veselago, Sov. Phys. Usp. 10 (1968) 509.
[2] J.B. Pendry, A.J. Holden, W.J. Stewart, I. Youngs, Phys. Rev. Lett. 76 (1996) 4773.
[3] J.B. Pendry, A.J. Holden, D.J. Robbins, W.J. Stewart, IEEE Trans. Microwave Theory Tech. 47 (1999) 2075.
[4] R.A. Shelby, D.R. Smith, S. Schultz, Science 292 (2001) 77.
[5] T.J. Yen, W.J. Padilla, N. Fang, D.C. Vier, D.R. Smith, J.B. Pendry, D.N. Basov, X. Zhang, Science 303 (2004) 1494.
[6] S. Linden, C. Enkrich, M. Wegener, J. Zhou, T. Koschny, C.M. Soukoulis, Science 306 (2004) 1351.
[7] A.N. Grigorenko, A.K. Geim, H.F. Gleeson, Y. Zhang, A.A. Firsov, I.Y. Khrushchev, J. Petrovic, Nature 438 (2005) 335.
[8] R. Marques, F. Medina, R. Rafii-El-Idrissi, Phys. Rev. B 65 (2002) 144440.
[9] N. Katsarakis, T. Koschny, M. Kafesaki, Appl. Phys. Lett. 84 (2004) 2943.
[10] L. Kang, C.R. Luo, Q. Zhao, J. Song, Q.H. Fu, X.P. Zhao, Chin. Sci. Bull. 49 (2004) 2440.
[11] Q. Zhao, X.P. Zhao, L. Kang, Acta Phys. Sin. 53 (2004) 2206.
[12] L. Kang, Q. Zhao, X.P. Zhao, Acta Phys. Sin. 53 (2004) 3379.
[13] C.R. Luo, L. Kang, Q. Zhao, Q.H. Fu, J. Song, X.P. Zhao, Acta Phys. Sin. 54 (2005) 1607.
[14] X.P. Zhao, Q. Zhao, L. Kang, J. Song, Q.H. Fu, Phys. Lett. A 346 (2005) 87.
[15] H. Liu, X.P. Zhao, Q.H. Fu, Solid State Commun. 140 (2006) 9.
[16] D.R. Smith, W.J. Padilla, D.C. Vier, S.C. Nemat-Nasser, S. Schultz, Phys. Rev. Lett. 84 (2000) 4184.
[17] T. Koschny, M. Kafesaki, E.N. Economou, C.M. Soukoulis, Phys. Rev. Lett. 93 (2004) 107402.
[18] D.R. Smith, S. Schultz, P. Markos, C.M. Soukoulis, Phys. Rev. B 65 (2002) 195104.
[19] X.D. Chen, T.M. Grzegorczyk, B.-I. Wu, J. Pacheco, J.A. Kong, Phys. Rev. E 70 (2004) 016608.
[20] D.H. Werner, R. Mittra, Frontiers in Electromagnetics, IEEE Press, Piscataway, NJ, 2000, pp. 732–768 (Chapter 18).
[21] A. Alu, A. Salandrino, N. Engheta, Opt. Express 14 (2006) 1557.
[22] M. Kafesaki, T. Koschny, R.S. Penciu, T.F. Gundogdu, E.N. Economou, C.M. Soukoulis, J. Opt. A: Pure Appl. Opt. 7 (2005) 12.
[23] D.R. Smith, D.C. Vier, T. Koschny, C.M. Soukoulis, Phys. Rev. E 71 (2005) 036617.
[24] L.D. Landau, E.M. Lifshitz, L.P. Pitaevskii, Electrodynamics of Continuous Media, Butterworth Heinenann, Oxford, 1984, pp. 329–367 (Chapter 9).